Design of Composite Filters with Equiripple Passbands and Least-Squares Stopbands

Wu-Sheng Lu
Dept. of Electrical and Computer Engineering
University of Victoria
Victoria, BC, Canada
Email: wslu@ece.uvic.ca

Takao Hinamoto
Hiroshima University
Higashi-Hiroshima, 739-8527, Japan
Email: hinamoto@ieee.org

***Abstract*—We study a class of composite filters (C-filters), each is composed of a prototype filter and a shaping filter in cascade, where the shaping filter is constructed by cascading several complementary comb filters. In particular, the problem of designing a C-filter with equiripple passband and least-squares stopband subject to peak stopband gain is formulated and an algorithm for designing such a class of linear-phase FIR C-filters is proposed. The algorithm is based on an alternating convex optimization strategy in that the prototype and shaping filters are optimized in separate steps which are coupled and carried out in a sequential manner to yield a satisfactory design. Design example is presented to illustrate the algorithm and demonstrate the performance of the C-filter relative to its conventional FIR counterparts.**

I. Introduction

A composite filter (C-filter) refers to a digital filtering system that is composed of explicit individual modules, often called subfilters, which are connected in cascade or parallel, or a mixture of both. Well known classes of C-filters include interpolated FIR filters [1][2], frequency-response-masking filters [3], and their variants, see e.g. [4]. Over the years, analysis and design of C-filters have attracted a great deal of research interest primarily because of their ability to offer improved computational efficiency relative to their conventional counterparts when appropriate subfilter structures are chosen and their parameters are optimized in accordance with certain design criterion [5]. Recently, C-filters composed of a prototype filter and a shaping filter, connected in cascade, are shown to offer certain advantages over conventional counterparts [6], [7]. In the case of FIR C-filters [6], the shaping filter is constructed by cascading several complementary comb filters (CCFs) of the form $(1 + z^{-l})^{k_l}$ with integers $1 \leq l \leq L$ and $k_l \geq 0$. As such, the shaping filter only requires several adders and memory units to implement and is free of multiplications. Yet, as demonstrated in [6], the shaping filter is capable of effectively improving filter performance, especially for those with narrow transition bands and highly suppressed stopbands.

In this paper, we present a new algorithm for the design of C-filters that assumes the same form $H(z) = H_p(z)H_s(z)$ as in [6], however prototype filter $H_s(z)$ as well as shaping filter $H_s(z)$ are designed through different approaches in order for $H(z)$ to achieve equiripple passbands and least-squares stopbands (EPLSS). EPLSS FIR filters, especially with narrow passbands, are desirable in wireless communications, aerospace systems, and synthetic aperture radar [8]. The design algorithm proposed in this paper uses a sequential optimization technique to deal with the design of $H_p(z)$ and $H_s(z)$ separately, yet these two design steps are coupled by alternately performing them. A strong motivation to develop such a design method is that both design steps can be formulated as convex problems hence can be solved efficiently. Numerical examples are presented to illustrate the design method and evaluate its performance.

II. Composite Filters and Problem Formulation

A. Composite filters

We consider a C-filter that is composed of two subfilters, known as prototype filter $H_p(z)$ and shaping filter $H_s(z)$ respectively, that are connected in cascade as shown in Fig. 1. Thus the transfer function of the C-filter assumes the form

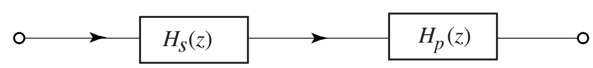

Fig. 1. A composite filter.

$$H(z) = H_p(z) \cdot H_s(z) \tag{1}$$

In this paper, we examine a class of linear-phase FIR C-filters where the prototype filter is an FIR filter of length N with transfer function

$$H_p(z) = \sum_{n=0}^{N-1} h_n z^{-n} \tag{2}$$

which largely determines the characteristics of $H(z)$, while the shaping filter is a CCF of the form

$$H_s(z) = \prod_{l=1}^{L} (1 + z^{-l})^{k_l} \tag{3}$$

where k_l are nonnegative integers, which reshapes the prototype filter for improved performance without substantial increase in implementation complexity.

For clarity of presentation, in the rest of the paper we focus on linear-phase lowpass FIR C-filters whose frequency response can be expressed as $H(\omega) = H_p(\omega)H_s(\omega)$ with

$$H_p(\omega) = \sum_{n=0}^{N-1} h_n e^{-jn\omega} = e^{-j\tau_p\omega}[\boldsymbol{x}^T \boldsymbol{c}(\omega)] \tag{4}$$

where $\tau_p = (N-1)/2$ is the group delay of $H_p(z)$, $\boldsymbol{x}$ is a coefficient vector determined by the impulse response of

$H_p(z)$, and $\boldsymbol{c}(\omega)$ is a vector with trigonometric components, and

$$H_s(\omega) = \prod_{l=1}^{L}(1+e^{-jl\omega})^{k_l} = e^{-j\tau_s\omega}\prod_{l=1}^{L}(2\cos\frac{l\omega}{2})^{k_l} \tag{5}$$

where $\tau_s = \frac{1}{2}\sum_{l=1}^{L} l\cdot k_l$. Therefore, the zero-phase frequency response of the C-filter is given by

$$A(\omega) = A_p(\omega)\cdot A_s(\omega) = \boldsymbol{x}^T\boldsymbol{c}(\omega)\prod_{l=1}^{L}(2\cos\frac{l\omega}{2})^{k_l} \tag{6}$$

and the group delay of the C-filter is given by $\tau = \tau_p + \tau_s$.

The behaviour of shaping filter $H_s(z)$ is determined by the number L of CCFs used and the power k_l for each CCF. As long as $k_l > 0$, the first notch of a single CCF $(1+z^{-l})^{k_l}$ over the normalized baseband $[0,\ \pi]$ occurs at $\omega = \pi/l$, see for example Fig. 2(a) for $(1+z^{-4})$ (a scaling factor 0.5 has been used in the figure to normalize the filter gain at $\omega = 0$ to unity). By cascading several CCFs with appropriate powers k_l, a shaping filter can offer much reduced stopband energy while retaining decent passband gain. As an example, Fig. 2(b) depicts the amplitude response of a shaping filter $H_s(z)$ with $L = 4$ and $\{k_l,\ l = 1,2,3,4\} = \{4,4,1,2\}$ where the filter gain at $\omega = 0$ has been normalized to unity.

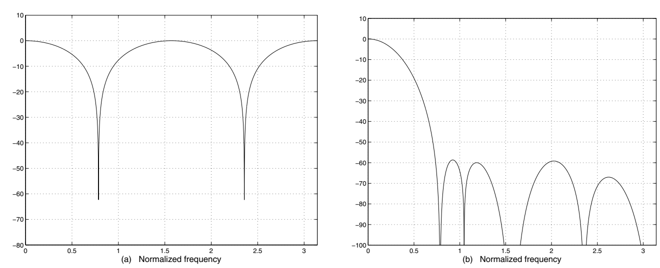

Fig. 2. Amplitude response of (a) $1+z^{-4}$ and (b) $(1+z^{-1})^4(1+z^{-2})^4(1+z^{-3})^1(1+z^{-4})^2$.

B. Problem formulation

Given a desired lowpass frequency response $H_d(\omega)$, prototype filter length N, and number of CCF's L, we seek to find a linear-phase FIR C-filter of form (1)–(3) such that the peak-to-peak amplitude ripple in passband is minimized subject to constraints on filter's energy as well as peak gain in stopband and total group delay τ. Note that the constraints imposed here would lead to an enhanced EPLSS C-filter in which largest peak in the stopband is under control and, in addition, the group delay is bounded so as to ensure its utility in on-line applications. The design objective is achieved by solving the constrained problem

$$\underset{\boldsymbol{x},\boldsymbol{y}}{\text{minimize}} \quad \max_{\omega\in\Omega_p}|H(\omega)-H_d(\omega)| \tag{7a}$$

$$\text{subject to:} \quad \int_{\omega_a}^{\pi}|H(\omega)|^2 d\omega \le e_a \tag{7b}$$

$$\max_{\omega\in\Omega_a}|H(\omega)| \le \delta_a \tag{7c}$$

$$\frac{1}{2}\sum_{l=1}^{L} l\cdot k_l \le D \tag{7d}$$

where Ω_p and Ω_a denote the passband and stopband, respectively, ω_a denotes the stopband edge, $\boldsymbol{x}$ from (4) and $\boldsymbol{y} = [k_1\ k_2\ \ldots\ k_L]^T$ are design variables, $e_a,\ \delta_a$ and D are constants representing upper bounds for stopband energy, peak filter gain in stopband, and group delay of the shaping filter, respectively. Note that the constraint in (7d) implies an upper bound $(N-1)/2+D$ for the total group delay of the C-filter.

III. Design Method

A. Design strategy

From (6), we see that design variables $\boldsymbol{x}$ and $\boldsymbol{y}$ are separate from each other. Moreover, frequency response $A(\omega)$ depends on $\boldsymbol{x}$ linearly, but on $\boldsymbol{y}$ highly nonlinearly. In addition, all components of variable $\boldsymbol{y}$ are constrained to be nonnegative integers. Under these circumstances, it is intuitively natural to optimize these design variables separately in an alternate fashion. This leads to a sequential procedure where in each step one of the variables, say $\boldsymbol{x}$, is optimized while the other variable, $\boldsymbol{y}$, is held fixed, and the solution so produced, say $\boldsymbol{x}_k$, is held fixed in the next step when variable $\boldsymbol{y}$ is updated to $\boldsymbol{y}_{k+1}$. The alternating optimization continues until a stopping criterion is met and the last pair of solutions $(\boldsymbol{y}_K, \boldsymbol{x}_K)$ is taken to be the optimal design. The rest of this section is devoted to describing the technical details involved in the design procedure.

B. Solving (7) with $\boldsymbol{y}$ fixed to $\boldsymbol{y} = \boldsymbol{y}_k$

With a fixed $\boldsymbol{y}$ that satisfies (7d), constraint (7d) can be neglected. By introducing an upper bound δ_p for the objective function as an auxiliary variable, the problem at hand becomes

$$\text{minimize} \quad \delta_p \tag{8a}$$

$$\text{s.t.} \quad |H(\omega)-H_d(\omega)| \le \delta_p \quad \text{for } \omega\in\Omega_p \tag{8b}$$

$$\int_{\omega_a}^{\pi}|H(\omega)|^2 d\omega \le e_a \tag{8c}$$

$$|H(\omega)| \le \delta_a \quad \text{for } \omega\in\Omega_a \tag{8d}$$

If the desired frequency response assumes the form $H_d(\omega) = e^{-j\tau\omega}A_d(\omega)$, then constraints in (8b)–(8d) are reduced to

$$|\boldsymbol{x}^T\hat{\boldsymbol{c}}(\omega) - A_d(\omega)| \le \delta_p \qquad \text{for } \omega\in\Omega_p \tag{9a}$$

$$\boldsymbol{x}^T\boldsymbol{Q}\boldsymbol{x} \le e_a \tag{9b}$$

$$|\boldsymbol{x}^T\hat{\boldsymbol{c}}(\omega)| \le \delta_a \qquad \text{for } \omega\in\Omega_a \tag{9c}$$

where

$$\hat{\boldsymbol{c}}(\omega) = \boldsymbol{c}(\omega)\prod_{l=1}^{L}(2\cos\frac{l\omega}{2})^{k_l}$$

and

$$\boldsymbol{Q} = \int_{\omega_a}^{\pi}\hat{\boldsymbol{c}}(\omega)\hat{\boldsymbol{c}}^T(\omega)\ d\omega$$

In realistic implementation, one has to deal with a finite set of constraints and this is accomplished by replacing sets Ω_p and Ω_a with their discrete counterparts $\hat{\Omega}_p = \{\omega_{p1},\ \omega_{p_2},\ \ldots,\ \omega_{pK_1}\}$ and $\hat{\Omega}_a = \{\omega_{a1},\ \omega_{a_2},\ \ldots,\ \omega_{aK_2}\}$ respectively, with the frequency grids placed uniformly over the respective bands. This simplifies problem (8) to

$$\begin{aligned} \text{minimize} \quad & \delta_p && \text{(10a)} \\ \text{s.t.} \quad & |\boldsymbol{x}^T \hat{\boldsymbol{c}}(\omega) - A_d(\omega)| \le \delta_p \quad \text{for } \omega \in \hat{\Omega}_p && \text{(10b)} \\ & \boldsymbol{x}^T \boldsymbol{Q} \boldsymbol{x} \le e_a && \text{(10c)} \\ & |\boldsymbol{x}^T \hat{\boldsymbol{c}}(\omega)| \le \delta_a \quad \text{for } \omega \in \hat{\Omega}_a && \text{(10d)} \end{aligned}$$

With respect to variables $(\delta_p, \boldsymbol{x})$, the objective function and constraints (10b) and (10d) are linear, while (10c) is a convex quadratic constraint because $\boldsymbol{Q}$ is positive definite. As a result, (10) is a convex problem whose global solution can be computed using reliable and convenient solvers [9], [10]. We denote the solution of (10) by $(\delta_k, \boldsymbol{x}_k)$.

C. Updating $\boldsymbol{y}$ with $\boldsymbol{x}$ fixed to $\boldsymbol{x} = \boldsymbol{x}_k$

Consider the stopband energy given by

$$J(\boldsymbol{y}) = \int_{\omega_a}^{\pi} |H(\omega)|^2 d\omega = \int_{\omega_a}^{\pi} |\boldsymbol{x}^T \boldsymbol{c}(\omega)|^2 \prod_{l=1}^{L} (4\cos^2 \frac{l\omega}{2})^{k_l} d\omega \tag{11}$$

where $\boldsymbol{x} = \boldsymbol{x}_k$ is obtained by solving (10) and is fixed throughout this step. Our strategy to update $\boldsymbol{y}$ is via minimizing $J(\boldsymbol{y})$ with respect to $\boldsymbol{y}$ subject to several relevant constraints on $\boldsymbol{y}$.

A technical difficulty to utilize continuous optimization to optimize $\boldsymbol{y}$ is that the components of y, must be integers. This problem is overcome by extending the k_l's from the domain of nonnegative integers to that of nonnegative reals. When an optimizing $\boldsymbol{y}$ with non-integer components is obtained, an integer solution can be found by rounding its components to nearest integers.

The gradient and Hessian of $J(\boldsymbol{y})$ are evaluated by computing

$$\frac{\partial J(\boldsymbol{y})}{\partial k_i} = \int_{\omega_a}^{\pi} |H(\omega)|^2 \cdot \log(4\cos^2 \frac{i\omega}{2}) d\omega$$

$$\frac{\partial^2 J(\boldsymbol{y})}{\partial k_i \partial k_j} = \int_{\omega_a}^{\pi} |H(\omega)|^2 \log(4\cos^2 \frac{i\omega}{2}) \log(4\cos^2 \frac{j\omega}{2}) d\omega$$

Note that with an arbitrary column vector $\boldsymbol{v}$ of length L

$$\boldsymbol{v}^T \nabla^2 J(\boldsymbol{y}) \boldsymbol{v} = \int_{\omega_a}^{\pi} |H(\omega)|^2 \left(\sum_{i=1}^{n} v_i \log(4\cos^2 \frac{i\omega}{2}) \right)^2 d\omega \ge 0$$

hence $J(\boldsymbol{y})$ is *convex* although it is a rather complicated function as shown in (11). This motivates a convex quadratic approximation of $J(\boldsymbol{y})$ as

$$\hat{J}(\boldsymbol{y}, \boldsymbol{y}_k) = J(\boldsymbol{y}_k) + \boldsymbol{d}_k^T \nabla J(\boldsymbol{y}_k) + \frac{1}{2} \boldsymbol{d}_k^T \nabla^2 J(\boldsymbol{y}_k) \boldsymbol{d}_k$$

where $\boldsymbol{d}_k = \boldsymbol{y} - \boldsymbol{y}_k$. We update $\boldsymbol{y}$ by minimizing $\hat{J}(\boldsymbol{y}, \boldsymbol{y}_k)$ subject to several constraints. These include an upper bound on group delay τ as seen in (7d) and nonnegativeness of the components of $\boldsymbol{y}$. An additional constraint is imposed to ensure the performance of the C-filter over the passband, especially at passband edge ω_p:

$$1 - d_p \le |H(\omega)|_{\omega=\omega_p} = |\boldsymbol{x}_k^T \boldsymbol{c}(\omega_p)| \prod_{l=1}^{L} |2\cos \frac{l\omega_p}{2}|^{k_l} \le 1 + d_p$$

with a small $d_p > 0$. This constraint is highly nonlinear w.r.t. $\boldsymbol{y}$, but fortunately it is equivalent to

$$\log(1 - d_p) \le c + \sum_{l=1}^{L} k_l \log|2\cos \frac{l\omega_p}{2}| \le \log(1 + d_p) \tag{12}$$

with $c = \log|\boldsymbol{x}_k^T \boldsymbol{c}(\omega_p)|$, which is *linear* with respect to $\boldsymbol{y}$. Based on above analysis, we propose to update $\boldsymbol{y}$ by solving the *convex* problem

$$\begin{aligned} \text{minimize} \quad & \frac{1}{2} (\boldsymbol{y} - \boldsymbol{y}_k)^T \nabla^2 J(\boldsymbol{y}_k)(\boldsymbol{y} - \boldsymbol{y}_k) \\ & + (\boldsymbol{y} - \boldsymbol{y}_k)^T \nabla J(\boldsymbol{y}_k) && \text{(13a)} \\ \text{subject to:} \quad & \text{(7d)},\ \boldsymbol{y} \ge \boldsymbol{0},\ \text{and (12)} && \text{(13b)} \end{aligned}$$

and then rounding its solution to a nearest integer solution $\boldsymbol{y}_{k+1}$.

D. Summary of the algorithm

The algorithm described above is outlined as Algorithm 1.

Algorithm 1 for C-Filters

Step 1 input $\boldsymbol{y}_0, (N, L, D), \omega_p, \omega_a, \delta_a, e_a, d_p,$ and K.
Step 2 for $k = 0,\ 1,\ \ldots$
(i) fix $\boldsymbol{y} = \boldsymbol{y}_k$ and solve (10) for $\boldsymbol{x}_k$;
(ii) fix $\boldsymbol{x} = \boldsymbol{x}_k$, perform K iterations of (13) for $\boldsymbol{y}_{k+1}$;
(iii) if $\boldsymbol{y}_k \ne \boldsymbol{y}_{k+1}$, set $k = k + 1$ and repeat from Step (i), otherwise go to Step 3.
Step 3 output $\boldsymbol{x}^* = \boldsymbol{x}_k,\ \boldsymbol{y}^* = \boldsymbol{y}_k$.

We remark that because both (10) and (13) are convex problems, globally optimal iterates $\boldsymbol{x}_k$ and $\boldsymbol{y}_k$ can be calculated efficiently.

Since the objective function in (13a) represents the filter's stopband energy, minimizing it tends to increase some powers in the shaping filter until the group delay of $H_s(z)$ reaches upper bound D in constraint (7d). When this occurs, iterate $\boldsymbol{y}_k$ remains unchanged and Algorithm 1 terminates.

IV. Design Example and Comparisons

We illustrate the design method proposed above by applying Algorithm 1 to design a narrow-band lowpass C-filter with linear phase response and sharp transition band specified by $\omega_p = 0.1\pi$ and $\omega_a = 0.11\pi$. The length of $H_p(z)$ was set to $N = 519$ and the peak gain of the C-filter in the stopband was set to be no greater than -60dB, i.e., $\delta_a = 0.001$.

The performance of the filters were evaluated in terms of peak-to-peak passband ripple A_p (in dB), minimum stopband attenuation A_a (in dB), stopband energy E_a, the number of multiplications M per output sample, and group delay τ. With $L = 7$, $D = 18$, $\boldsymbol{y}_0 = [1\ 1\ 1\ 1\ 1\ 1\ 1]^T$, $d_p = 0.08$, and

$e_a = 5 \times 10^{-4}$, problem (10) was solved and its solution $\boldsymbol{x}_0$ together with $\boldsymbol{y}_0$ defines a C-filter achieving $A_p = 0.1681$, $A_a = 60$, and $E_a = 2.15 \times 10^{-8}$. With $\boldsymbol{x}_0$ held fixed, $K = 5$ iterations of (13) were performed to obtain an integer solution $\boldsymbol{y}_1 = [1\ 1\ 1\ 1\ 1\ 1\ 2]^T$. Since $\boldsymbol{y}_1 \neq \boldsymbol{y}_0$, problem (10) was solved again with $\boldsymbol{y}$ fixed to $\boldsymbol{y}_1$, where e_a was adjusted in order obtain a solution $\boldsymbol{x}_1$ with practically the same peak gain in the stopband and stopband energy as $\boldsymbol{x}_0$ so that the two iterates $\boldsymbol{x}_0$ and $\boldsymbol{x}_1$ can be compared with each other in terms of peak passband ripple. With $e_a = 2.95 \times 10^{-4}$, the C-filter specified by $(\boldsymbol{x}_1, \boldsymbol{y}_1)$ achieved $A_p = 0.1389$, $A_a = 60.04$ and $E_a = 2.12 \times 10^{-8}$. We then run (13) again with $\boldsymbol{x}$ fixed to $\boldsymbol{x}_1$ and $K = 5$, this yields an integer solution $\boldsymbol{y}_2 = [1\ 1\ 1\ 1\ 1\ 1\ 2]^T$. Since $\boldsymbol{y}_2 = \boldsymbol{y}_1$, the algorithm is terminated and $(\boldsymbol{x}_1, \boldsymbol{y}_1)$ is claimed as the solution. The amplitude responses of $H_p(z)$ and $H(z)$ are shown in Fig.3(a) and (b), respectively, and the amplitude response of $H(z)$ in the passband is depicted in Fig.3(c).

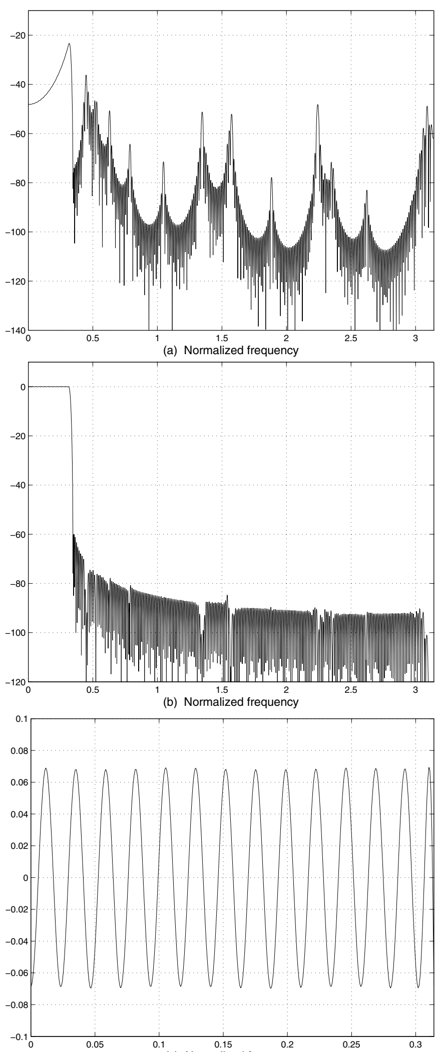

Fig. 3. Amplitude response of (a) the prototype filter $H_p(z)$, (b) the C-filter $H(z)$ and (c) the C-filter $H(z)$ over the passband.

The filters that are most relevant to the C-Filters addressed in this paper are linear-phase EPLSS FIR filters with constrained peak gain in stopband and linear-phase FIR filters with equiripple passbands and stopbands obtained using the Parks-McClellan (P-M) algorithm. For comparison purposes, an EPLSS lowpass filter and a P-M lowpass filter with the same ω_p and ω_a as those in the C-filter were designed, both satisfy the same peak stopband gain of -60 dB as the C-filter. The evaluation results are summarized in Table I.

TABLE I
COMPARISONS OF C-FILTER WITH EPLSS AND P-M FILTERS

Filters	N	A_p	A_a	E_a	M	τ
C-filter	**519**	**0.1389**	**60.04**	$\mathbf{2.12 \times 10^{-8}}$	**260**	277.5
EPLSS	551	0.1465	60.03	2.13×10^{-8}	276	275
P-M	531	0.1463	60.03	1.36×10^{-6}	266	**265**

It is observed that the C-filter outperforms the two conventional filters at the cost of a slight increase in group delay. Relative to the EPLSS filter, the C-filter offers reduced passband ripple and requires less number of multiplications for implementation. On comparing with the P-M filter, the C-filter also offers smaller passband ripple, reduced number of multiplications, and considerably smaller stopband energy.

V. Conclusion

We have addressed the design of a class of composite filters by an alternating convex optimization strategy to achieve equiripple passband and least-squares stopband subject to peak-gain constraint. A design example is presented to illustrate the proposed algorithm and to demonstrate the performance of C-filter relative to the conventional EPLSS and P-M filters.

References

[1] Y. Neuvo, C. Y. Dong, and S. K. Mitra, "Interpolated finite impulse response filters," *IEEE Trans. Acoust., Speech, Signal Process.*, vol. ASSP-32, pp. 563–570, Jun. 1984.

[2] T. Saramäki, Y. Neuvo, and S. K. Mitra, "Design of computationally efficient interpoted FIR filters," *IEEE Trans. Circuits Syst.*, vol. 35, pp. 70–88, Jan. 1988.

[3] Y. C. Lim, "Frequency-response masking approach for the synthesis of sharp linear phase digital filters," *IEEE Trans. Circuits Syst.*, vol. 33, pp. 357–364, Apr. 1986.

[4] W.-S. Lu and T. Hinamoto, "A unified approach to the design of interpolated and frequency-response-masking FIR filters," to appear in *IEEE Trans. Circuits Syst. I*, 2016.

[5] S. K. Mitra, *Digital Signal Processing – A Computer-Based Approach*, 3rd ed., McGraw Hill, 2006.

[6] D. Shiung, Y.-Y. Yang, and C.-S. Yang, "Improving FIR filters by using cascade techniques," *IEEE Signal Processing Mag.*, vol. 33, pp. 108–114, May 2016.

[7] D. Shiung, Y.-Y. Yang, and C.-S. Yang, "Cascading tricks for designing composite filters with sharp transition bands," *IEEE Signal Processing Mag.*, vol. 33, no. 1, pp. 151–157 and 162, Jan. 2016.

[8] J. W. Adams, "FIR digital filters with least-squares stopbands subject to peak-gain constraints," *IEEE Trans. Circuits Syst.*, vol. 39, no. 4, pp. 376–388, Apr. 1991.

[9] SeDuMi1.3: http://sedumi.ie.lehigh.edu/

[10] CVX2.1: http://cvxr.com/cvx/